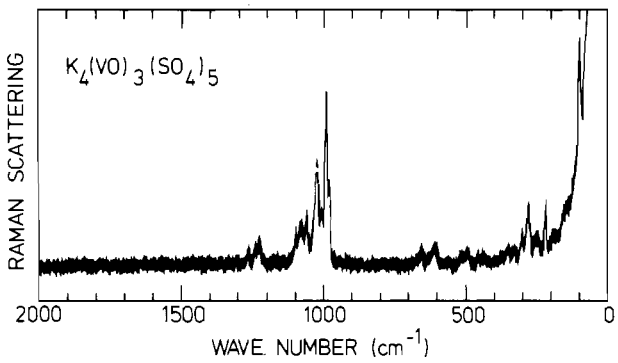

Figure 9. Raman spectra of $K_4(VO)_3(SO_4)_5$ powder at room temperature ($\lambda_0 \sim 488.0$ nm; power ~ 100 mW; resolution ~ 2 cm^{-1}).

Infrared Spectra. IR spectra of blue $K_4(VO)_3(SO_4)_5$ at room temperature (see Figure 8) were obtained on finely ground powders in pressed KBr disks. The IR band positions and tentative assignments are given in the supplementary material. The characteristic V=O stretching[26] at ca. 975 cm^{-1} on top of the presence of many bands in the sulfate stretching region (ca. 1200-1000 cm^{-1}) and the complete absence of bands[2] that might be due to $S_2O_7^{2-}$ should be noted.

Raman Spectra. Raman spectra were obtained at room temperature on stationary polycrystalline samples (Figure 9); the bands observed are listed and tentative assignments are given in the supplementary material (Table C).

Discussion. As can be seen from Figures 8 and 9, the IR and Raman spectra contain many bands and most of them are common to both kinds of spectra. This is in accordance with what is to be expected from a unit cell containing as many as three VO and five SO_4 groups in a low symmetry. Sulfate groups under various crystal environments were recently studied, and similar band-rich spectra were seen.[38] In infrared spectra of V(IV) compounds in analogous frozen-melt systems, similar features have been observed.[11,12,37] Probably, blue V(IV) compounds were formed in these SO_2-reduced systems, but the procedures of freezing the melts did not permit an isolation of pure samples, e.g. of $K_4(VO)_3(SO_4)_5$.

Conclusion

The compound $K_4(VO)_3(SO_4)_5$ has been isolated from $V_2O_5/K_2S_2O_7/SO_2$ melts, and its molecular structure was determined.

The deactivation of sulfuric acid catalysts at lower temperatures has been attributed[9,10,39,40] to the precipitation of V(IV) compounds. Furthermore, work in progress[14] shows that the compound $K_4(VO)_3(SO_4)_5$ is formed in the $V_2O_5/K_2S_2O_7$-$SO_2/O_2/N_2$ liquid-gas system, and simultaneously, a dramatic decrease in the catalytic activity of the system is seen. Thus, the precipitation of the V(IV) compound $K_4(VO)_3(SO_4)_5$ may account for the observed deactivation of the commercial catalyst at low temperatures.

Acknowledgment. This investigation was in part supported by the "Stimulation Actions" program of the European Economic Community (EEC Contract No. STI-011-J-C(CD)).

Supplementary Material Available: Tables A, C, and D, listing temperature factor parameters, IR and Raman bands, and all crystallographic data (4 pages); Table B, listing observed and calculated structure factors (31 pages). Ordering information is given on any current masthead page.

(38) Bremard, C.; Laureyns, J.; Abraham, F. *J. Raman Spectrosc.* **1986**, *17*, 397.
(39) Kozyrev, S. V.; Balzhinimaev, B. S.; Boreskov, G. K.; Ivanov, A. A.; Mastikhin, V. M. *React. Kinet. Catal. Lett.* **1982**, *20*, 53.
(40) Borisov, V. M.; Berezkina, L. G.; Bel'skaya, N. P.; Gubareva, V. N.; Petrovskaya, G. I.; Pogodilova, E. G.; Stul', R. M. *Zh. Prikl. Khimii (Leningrad)* **1987**, *60*, 612. *J. Appl. Chem. USSR (Engl. Transl.)* **1987**, *60*, 575.

Contribution from the School of Chemistry, University of New South Wales, Kensington, NSW 2033, Australia

Monocyclic Copper and Silver Tertiary Alkanethiolates: Formation and Molecular Structures of $(CuSBu^t)_4(Ph_3P)_2$, $(AgSCMeEt_2)_8(Ph_3P)_2$, and $(AgSBu^t)_{14}(Ph_3P)_4$ and Structural Principles

Ian G. Dance,* Lyn J. Fitzpatrick, Donald C. Craig, and Marcia L. Scudder

Received August 19, 1988

The molecular compounds $(CuSBu^t)_4(Ph_3P)_2$ (**8**), $(AgSCMeEt_2)_8(Ph_3P)_2$ (**9**), and $(AgSBu^t)_{14}(Ph_3P)_4(CHCl_3)_2$ (**10**), formed by reactions of the nonmolecular metal tertiary alkanethiolates with triphenylphosphine, have been characterized by crystal structure determinations. The single cycle in **8** contains alternating segments of linear $(\mu\text{-SR})Cu^{dig}(\mu\text{-SR})$ and trigonal $(\mu\text{-SR})_2Cu^{trig}(PPh_3)$. **9** contains two different tetrasilver cycles, one $((\mu\text{-SCMeEt})_4(Ag^{dig})_4)$ with digonal silver only, and the other $((\mu\text{-SCMeEt}_2)_4(Ag^{dig})_2(Ph_3PAg^{trig})_2)$ with Ph_3P ligands on two opposite trigonal metal atoms: four long secondary interactions connect the two cycles. A much larger 28-membered cycle of alternating silver and sulfur atoms occurs in **10**, with the phosphine ligands on Ag^{trig} atoms 1, 6, 8, and 13. The cycle is folded such that its digonal and trigonal segments lie approximately in the faces of a box, with virtual symmetry C_{2h}. There are four types of segments in **10**: (i) eight opposed zigzag linear segments in opposite faces of the box; (ii) four linear crossover segments on another pair of faces; (iii) four trigonal bending segments, which connect to (iv) two linear end segments, one in each end of the box. Structural features that occur in these three compounds, as well as four other compounds with related but different structures, permit extraction of structural principles for copper(I) and silver(I) thiolate complexes with branched-chain alkyl substituents. Crystal data: **8**, $C_{52}H_{66}Cu_4S_4P_2$, space group $P2_1/c$, $a = 13.213$ (6) Å, $b = 27.242$ (8) Å, $c = 20.601$ (8) Å, $\beta = 130.57$ (1)°, $V = 5632$ (4) Å^3, $Z = 8$, 4068 observed ($I > 3\sigma(I)$) reflections (Mo Kα), $R = 0.045$; **9**, $C_{84}H_{134}Ag_8S_8P_2$, space group $P2_1/c$, $a = 14.736$ (8) Å, $b = 27.108$ (4) Å, $c = 24.94$ (2) Å, $\beta = 99.85$ (3)°, $V = 9815$ (8) Å^3, $Z = 4$, 5067 observed ($I > 3\sigma(I)$) reflections (Mo Kα), $R = 0.057$; **10**, $C_{128}H_{186}Ag_{14}S_{14}P_4(CHCl_3)_2$, space group $P\bar{1}$, $a = 13.523$ (8) Å, $b = 13.852$ (7) Å, $c = 21.808$ (12) Å, $\alpha = 79.86$ (4)°, $\beta = 86.08$ (4)°, $\gamma = 85.75$ (4)°, $V = 4004$ (4) Å^3, $Z = 1$, 2690 observed ($I > 3\sigma(I)$) reflections (Mo Kα), $R = 0.067$.

Introduction

Alkane- and arenethiolate compounds MSR of copper and silver are still incompletely characterized structurally, largely due to difficulties with insolubility and poor crystal habit, and there are only a few crystal structure determinations for this long-known class of compounds.[1] One approach to the problem has been to increase the steric bulk of the substituent R. Åkerström showed that multiple branching and bulk in the thiolate substituent enhanced the solubilities of $(MSR)_p$ in inert solvents and determined from ebullioscopic molecular weight measurements that silver

(1) Dance, I. G. *Polyhedron* **1986**, *5*, 1037.

0020-1669/89/1328-1853$01.50/0 © 1989 American Chemical Society

Table I. Crystallographic Details for **8–10**

	8	**9**	**10**
formula	$C_{52}H_{66}Cu_4S_4P_2$	$Ag_8S_8C_{84}H_{134}P_2$	$C_{128}H_{186}Ag_{14}S_{14}P_4(CHCl_3)_2$
formula mass	1134.86	2325.4	4046.6
space group	$P2_1/c$	$P2_1/c$	$P\bar{1}$
a/Å	13.213 (6)	14.736 (8)	13.523 (8)
b/Å	27.242 (8)	27.108 (4)	13.852 (7)
c/Å	20.601 (8)	24.94 (2)	21.808 (12)
α/deg	90	90	79.86 (4)
β/deg	130.57 (1)	99.85 (3)	86.08 (4)
γ/deg	90	90	85.75 (4)
V/Å^3	5632 (4)	9815 (8)	4004 (4)
temp/°C	21 (1)	21 (1)	21 (1)
D_{obs}/g cm^{-3}			1.69 (2)
Z	8	4	1
D_{calc}/g cm^{-3}	1.34	1.57	1.68
radiation; λ/Å	Mo Kα, 0.7107	Mo Kα; 0.7107	Mo Kα; 0.7107
μ/cm^{-1}	17.24	17.8	20.1
$R = \sum^m\|\Delta F\|/\sum^m\|F_o\|$	0.045	0.057	0.067
$R_w = [\sum^m w\|\Delta F\|^2/\sum^m w\|F_o\|^2]^{1/2}$	0.054	0.073	0.090
transmiss coeff	0.64–0.80	0.66–0.71	0.65–0.78

tertiary alkanethiolates are generally octameric ($p = 8$) in solution, while silver secondary alkanethiolates have p = 12.[2] By this technique the crystal structures of $(AgSC_6H_{11})_{12}$ (**1**)[3,4] and $[AgSCMeEt_2]_\infty$ (**2**)[5] were obtained. Crystalline **2** is one-dimen-

2

sionally nonmolecular, with two intertwined (but nonbonded) strands in the chain, and a mechanism for interconversion of the crystal structure and the octameric molecules in solution has been proposed.[5] More recently the same approach has led to crystal structure determinations[6] for $[AgSC(SiMe_3)_3]_4$ (**3**), $[AgSC(SiMe_2Ph)_3]_3$ (**4**), $[AgSCH(SiMe_3)_2]_8$ (**5**), and $[Ag_4\{SCH_2(SiMe_3)\}_3(OMe)]_\infty$ (**6**).

Another method for circumventing the crystallographic obstinance of nonmolecular metal thiolates is to react them with small proportions of heteroligands that are bulky and structure terminating, with the presumption that the resulting molecular structures represent fragments of the nonmolecular lattice. For example, the product of the reaction of $[CuSCMe_2Et]_\infty$ with CS_2 is $Cu_8(SCMe_2Et)_4(S_2CSCMe_2Et)_4$, the structure of which[7] has been interpreted[8] in terms of one-dimensionally nonmolecular structures for $[CuSR]_\infty$. Tertiary phosphines are excellent structure-terminating ligands, and we have determined the structures of the following copper and silver arenethiolate derivatives with triphenylphosphine: $Ag_6(SAr)_6(PPh_3)_5$,[9] $Cu_4(SPh)_4(PPh_3)_4$ (**7**).[10] $Cu_3(SAr)_3(PPh_3)_4$ (Ar = C_6H_5,[11] C_6H_4Cl-4), and $Cu_2(SAr)_2(PPh_3)_4$.[12]

Our investigations have extended to phosphines as terminating ligands also for copper and silver alkanethiolates, and we here report and interpret the structures of the three compounds $(CuSBu^t)_4(Ph_3P)_2$ (**8**), $(AgSCMeEt_2)_8(Ph_3P)_2$ (**9**), and $(AgSBu^t)_{14}(Ph_3P)_4$ (**10**), formed with tertiary alkanethiolates and triphenylphosphine. Also presented here are the structural principles derived from the patterns observed in these and related structures. Some of these results have been communicated briefly.[13]

Experimental Section

$AgSCMeEt_2$ was prepared as previously described.[5] All preparations were performed under dinitrogen, and in subdued light. The products are oxidized slowly by dioxygen and darken on exposure to sunlight.

$(CuSBu^t)_4(Ph_3P)_2$ (8). $CuSBu^t$ (0.5 g, 3.3 mmol) was added in small portions to a solution of triphenylphosphine (0.86 g, 3.3 mmol) in chloroform (10 mL) and stirred until dissolved. The solution was diluted with propanol and stored at 0 °C. The pale yellow crystals (0.5 g) that formed were collected after 4 days. Mp: 143–148 °C dec. Anal. Calcd for $Cu_4S_4P_2C_{52}H_{66}$: C, 55.00; H, 5.86. Found: C, 55.18; H, 5.86. The same product was obtained from a similar reaction in toluene.

$(AgSCMeEt_2)_8(Ph_3P)_2$ (9). A solution of triphenylphosphine (0.76 g, 3 mmol) in acetone (25 mL) was added to $AgSCMeEt_2$ (0.45 g, 2 mmol) and stirred in the dark. A small amount of solid that formed was dissolved by warming to 50 °C for 15 min, and after filtration the solution was stored at 0 °C. Pale yellow crystals (0.64 g) were collected after 24 h. Mp: 109–110 °C. Anal. Calcd for $Ag_8S_8P_2C_{134}H_{84}$: C, 43.39; H, 5.81. Found: C, 43.34; H, 6.28. A similar reaction in which the PPh_3/AgSR molar ratio was 1 yielded the same product. When this ratio was reduced to 0.5, the reaction mixtures crystallized (on different occasions) either the above product as large pale yellow crystals in high yield, or $AgSCMeEt_2$, which was identified by analysis, IR spectroscopy and melting point.

$(AgSBu^t)_{14}(Ph_3P)_4(CHCl_3)_2$ (10). A solution of triphenylphosphine (0.67 g, 2.5 mmol) in $CHCl_3$ (10 mL) was added to $AgSBu^t$ (0.5 g, 2.5 mmol) with warming and stirring for about 15 min. After addition of further $CHCl_3$ (10 mL) and filtration, propanol (20 mL) was added and the sealed mixture allowed to stand at ambient temperature. The first colorless crystalline product that separated (0.5 g, largely $AgSBu^t$ by X-ray diffraction) was filtered after 1 week, and the filtrate on storage at 0 °C slowly grew blocky colorless crystals of the product after about 8 weeks. The crystals were air dried, and characterized by X-ray crystallography. A small second crop was obtained. Similar reactions with PPh_3/$AgSBu^t$ molar ratios of 2/7, 0.5, 1.5, 2, and 3 yielded needles of $AgSBu^t$ as the crystalline product. Dissolution of $AgSBu^t$ does not occur in toluene solutions of triphenylphosphine. Evidently a large excess of triphenylphosphine, chloroform, and seeding are required to obtain crystallization of **10**. It was observed that **10** dissolved in or reacted with the mixture of iodobutane and 1,2-dibromoethane used in the density determination.

X-ray Crystallography. Intensity data were recorded for all three structures with a Nonius CAD4 diffractometer and monochromated Mo Kα radiation. Data collection and reduction were carried out as previously described[5] except that the ω scan was $(\delta + 0.35 \tan\theta)°$ with δ =

(2) (a) Åkerström, S. *Acta Chem. Scand.* **1964**, *18*, 1308. (b) Åkerström, S. *Arkiv for Kemi* **1965**, *24*, 505.
(3) Hong, S.-H.; Olin, Å.; Hesse, R. *Acta Chem. Scand.* **1975**, *A29*, 583.
(4) Dance, I. G. *Inorg. Chim. Acta* **1977**, *25*, L17.
(5) Dance, I. G.; Fitzpatrick, L. J.; Rae, A. D.; Scudder, M. L. *Inorg. Chem.* **1983**, *22*, 3785.
(6) Tang, K.; Aslam, M.; Block, E.; Nicholson, T.; Zubieta, J. *Inorg. Chem.* **1987**, *26*, 1488.
(7) Chadha, R.; Kumar, R.; Tuck, D. G. *J. Chem. Soc., Chem. Commun.* **1986**, 188.
(8) Dance, I. G. *Polyhedron* **1988**, *7*, 2205.
(9) Dance, I. G.; Fitzpatrick, L. J.; Scudder, M. L. *Inorg. Chem.* **1984**, *23*, 2276.
(10) Dance, I. G.; Fitzpatrick, L. J.; Scudder, M. L. *Inorg. Chem.* **1985**, *24*, 2547.
(11) Dance, I. G.; Fitzpatrick, L. J.; Scudder, M. L. *J. Chem. Soc., Chem. Commun.* **1983**, 546.
(12) Dance, I. G.; Guerney, P. J.; Rae, A. D.; Scudder, M. L. *Inorg. Chem.* **1983**, *22*, 2883.
(13) Dance, I. G.; Fitzpatrick, L. J.; Scudder, M. L.; Craig, D. C. *J. Chem. Soc., Chem. Commun.* **1984**, 17.

0.70, 0.60, and 0.80 for **8–10**, respectively. Calculated corrections for absorption were made, and in each case corrections were made for decomposition during data collection. Reflections with $I > 3\sigma(I)$ were regarded as observed. Weights $w = \sigma^2(F_o)$ were assigned to reflections with $\sigma(F_o)$ derived from $\sigma(F_o) = [\sigma(I_o) + (0.04I_o)^2]^{1/2}$. No corrections for extinction were made. Scattering factors, including $\Delta f'$ and $\Delta f''$ for Cu, Ag, S, and P were taken from ref 14. Numerical details pertaining to the crystal lattice, the collection of the diffraction data, and final refinement of the structures are listed partly in Table I and in fully in Table S1.[15] The solution and refinement of each structure is described below.

Structure of 8. The structure was solved by direct methods (MULTAN). The Cu, S, and P atoms were all located and included in a Fourier synthesis from which all remaining non-hydrogen atoms were located. Refinement including anisotropic thermal parameters for Cu, S, and P and isotropic temperature factors for all other atoms gave $R = 0.064$. The hydrogen atoms of the Bu^t groups were included at positions determined from a difference Fourier synthesis, and the H atoms of the PPh_3 groups were placed at calculated positions. All hydrogen atoms were assigned isotropic temperature factors equal to those of the atoms to which they were bound. Refinement was completed with the carbon atoms of the SBu^t group also having anisotropic thermal parameters and converged with $R = 0.045$.

Structure of 9. Five Ag atoms, two P atoms, and six S atoms were readily located by using direct methods (MULTAN), and the positions of the remaining non-hydrogen atoms were determined from successive Fourier syntheses. Some of the ligand side chains were difficult to parametrize. This may have been due to the occurrence of disordering, but attempts to define the disorder did not produce an improved model for their geometry. The hydrogen atoms of the PPh_3 groups were included in calculated positions with temperature factors equal to those of the atoms to which they were bonded. The structure was refined by using block-diagonal least-squares techniques, with the Ag, S, and P atoms having anisotropic temperature factors and the carbon atoms isotropic temperature factors. The final residual R was 0.057, and the larger peaks in the final difference map were ca. 0.8 e Å^{-3}; located in the vicinity of the Bu^t side chains.

Structure of 10. The positions of the seven Ag atoms were found by direct methods (MULTAN), and the remainder of the structure was determined by successive Fourier syntheses. In the final refinement, the Ag atoms were given anisotropic thermal parameters, while the remainder of the atoms were refined with isotropic temperature factors. Hydrogen atoms were not included. Refinement converged with $R = 0.067$. There were insufficient observed data to sustain more parameters in the refinement. The largest peaks in the final difference map were ca. 0.8 e Å^{-3} and were in the vicinity of the Ag atoms.

Atomic coordinates for the non-hydrogen atoms of **8–10** are presented in Tables II–IV, respectively. The atom labeling common to all structures is as follows: S*mn* bridges atoms Cu(Ag)*m* and Cu(Ag)*n*; the SBu^t ligands in **8** and **10** are S*mn*–C1*mn*–{C2*mn*, C3*mn*, C4*mn*}, while the $SCMeEt_2$ ligand in **9** is S*mn*–C1*mn*–{(C2*mn*–C3*mn*), (C4*mn*–C5*mn*), C6*mn*}; the rings of the PPh_3 ligands are labeled C11P*q*···C61P*q*, C12P*q*···C62P*q*, C13P*q*···C63P*q* (*q* = 1, 2). Full tabulations of all atomic parameters are available as supplementary material.[15]

Important bond lengths and angles for the three structures are displayed in Tables V–VII. Bond lengths and angles within the thiolate substituents and the phenyl substituents are unexceptional and are included with the supplementary material.

Results

Formation and Crystallization. The solubilities of tertiary alkanethiolates of copper and silver in inert solvents are enhanced by the addition of triphenylphosphine. However a substantial molar excess of phosphine in solution is required in order to crystallize the derivative, which contains a proportion of phosphine much smaller than that in solution. Thus, **8** with P/Cu = 0.5 crystallizes from solutions where this ratio is 1, **9** with P/Ag = 0.25 crystallizes only from solutions in which this ratio is 0.5, and **10** evidently requires an unknown large excess (P/Ag ≫ 1) in solution even though the crystalline compound has P/Ag = 0.29. It is recognized that the compositions and structures of the compounds isolated are not necessarily those of the species in the solutions from which they crystallized.

(14) Ibers, J. A., Hamilton, W. C., Eds. *International Tables for X-ray Crystallography*; Kynoch Press: Birmingham, England, 1974; vol IV, Tables 2.2A and 2.3.1.
(15) See paragraph at end of paper regarding supplementary material.

Table II. Positional Parameters for the Non-Hydrogen Atoms of **8**

atom	*x/a*	*y/b*	*z/c*
Cu1	0.3544 (1)	0.1763 (0)	0.0922 (1)
Cu2	0.6437 (1)	0.0686 (0)	0.3159 (1)
Cu3	0.3722 (1)	0.0922 (0)	0.1814 (1)
Cu4	0.6455 (1)	0.1588 (0)	0.2240 (1)
S13	0.2650 (2)	0.1600 (1)	0.1526 (1)
S23	0.4712 (2)	0.0219 (1)	0.2121 (1)
S24	0.7778 (2)	0.0978 (1)	0.2926 (1)
S14	0.5357 (2)	0.2256 (1)	0.1629 (1)
P1	0.2820 (2)	0.1576 (1)	−0.0385 (1)
P2	0.7270 (2)	0.0808 (1)	0.4507 (1)
C113	0.0852 (9)	0.1432 (3)	0.0829 (6)
C213	0.0090 (13)	0.1906 (5)	0.0446 (9)
C313	0.0463 (12)	0.1051 (7)	0.0250 (11)
C413	0.0609 (12)	0.1281 (5)	0.1409 (8)
C123	0.4006 (7)	−0.0205 (3)	0.2441 (5)
C223	0.3725 (8)	0.0053 (3)	0.2962 (5)
C323	0.5004 (10)	−0.0612 (3)	0.2957 (6)
C423	0.2721 (9)	−0.0407 (3)	0.1613 (6)
C124	0.7676 (7)	0.0623 (3)	0.2118 (4)
C224	0.8209 (9)	0.0111 (3)	0.2485 (5)
C324	0.6294 (8)	0.0584 (3)	0.1275 (5)
C424	0.8577 (9)	0.0877 (3)	0.2007 (6)
C114	0.5670 (9)	0.2625 (3)	0.2498 (5)
C214	0.4530 (12)	0.2966 (4)	0.2101 (7)
C314	0.5743 (14)	0.2310 (4)	0.3124 (7)
C414	0.6917 (11)	0.2913 (4)	0.2912 (7)
C11P1	0.1823 (8)	0.2072 (3)	−0.1126 (5)
C21P1	0.1251 (10)	0.2403 (4)	−0.0945 (6)
C31P1	0.0384 (12)	0.2774 (5)	−0.1534 (8)
C41P1	0.0077 (14)	0.2780 (5)	−0.2304 (9)
C51P1	0.0705 (16)	0.2479 (6)	−0.2462 (10)
C61P1	0.1573 (11)	0.2105 (4)	−0.1869 (7)
C12P1	0.4083 (7)	0.1473 (3)	−0.0488 (4)
C22P1	0.4073 (8)	0.1064 (3)	−0.0889 (5)
C32P1	0.5086 (9)	0.1005 (3)	−0.0926 (5)
C41P1	0.6063 (9)	0.1343 (3)	−0.0578 (5)
C52P1	0.6113 (9)	0.1749 (3)	−0.0165 (5)
C62P1	0.5081 (9)	0.1814 (3)	−0.0137 (5)
C13P1	0.1746 (7)	0.1041 (3)	−0.0893 (5)
C23P1	0.2204 (7)	0.0607 (3)	−0.0411 (5)
C33P1	0.1432 (8)	0.0187 (3)	−0.0733 (5)
C43P1	0.0202 (9)	0.0197 (3)	−0.1534 (5)
C53P1	−0.0260 (9)	0.0610 (4)	−0.2014 (6)
C63P1	0.0501 (8)	0.1046 (3)	−0.1700 (5)
C11P2	0.7511 (7)	0.0210 (3)	0.4989 (4)
C21P2	0.8282 (8)	−0.0129 (3)	0.4971 (5)
C31P2	0.8455 (9)	−0.0611 (4)	0.5282 (6)
C41P2	0.7830 (10)	−0.0741 (4)	0.5576 (6)
C51P2	0.7086 (10)	−0.0422 (4)	0.5612 (6)
C61P2	0.6912 (8)	0.0067 (3)	0.5309 (5)
C12P2	0.8927 (8)	0.1076 (3)	0.5230 (5)
C22P2	0.9224 (9)	0.1472 (3)	0.4967 (6)
C32P2	1.0481 (11)	0.1700 (4)	0.5522 (7)
C42P2	1.1414 (11)	0.1518 (4)	0.6313 (7)
C52P2	1.1156 (11)	0.1143 (4)	0.6603 (7)
C62P2	0.9882 (10)	0.0915 (4)	0.6053 (6)
C13P2	0.6340 (8)	0.1179 (3)	0.4698 (5)
C23P2	0.5061 (8)	0.1300 (3)	0.4033 (5)
C33P2	0.4284 (10)	0.1600 (4)	0.4129 (6)
C43P2	0.4871 (11)	0.1755 (4)	0.4931 (7)
C53P2	0.6077 (13)	0.1654 (4)	0.5577 (7)
C63P2	0.6932 (11)	0.1351 (4)	0.5523 (7)

Molecular Structures. Although **8–10** differ in composition and overall topology, they possess similarities of connectivity and local geometry. Figure 1 is a comparative diagrammatic representation of the atom labeling, connectivities, and dimensions of the asymmetric units of the three structures. We describe first the topology, conformation, and distinctive geometrical features of each molecule and then make a general comparative analysis.

Structure of 8. The cyclic molecular structure, shown in Figure 2, possesses no actual or virtual symmetry. All of the SBu^t ligands are pyramidal double bridges, and each links one linear digonal copper atom (Cu^{dig}) and one trigonal copper atom (Cu^{trig}) which also has a terminal PPh_3 ligand. The ring contains eight atoms, but because there are two linear segments, its conformation can

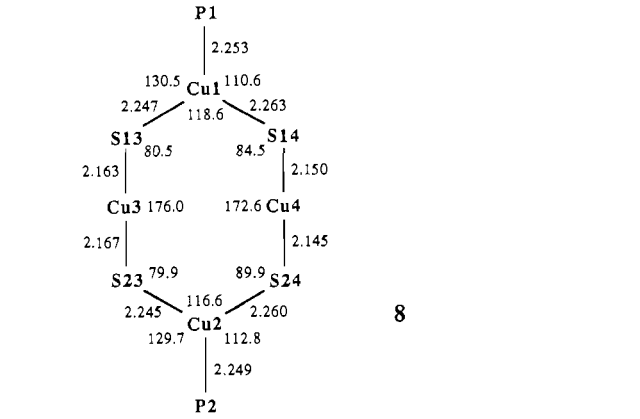

8

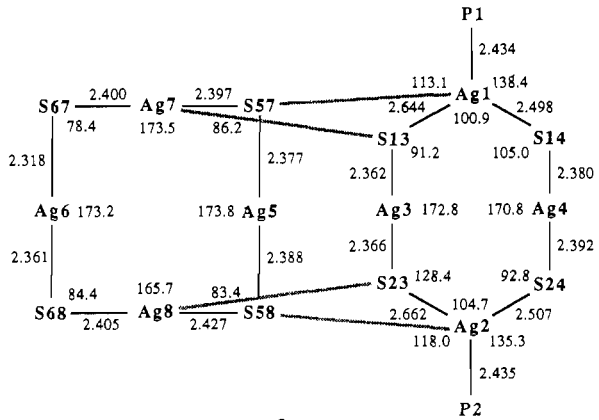

9

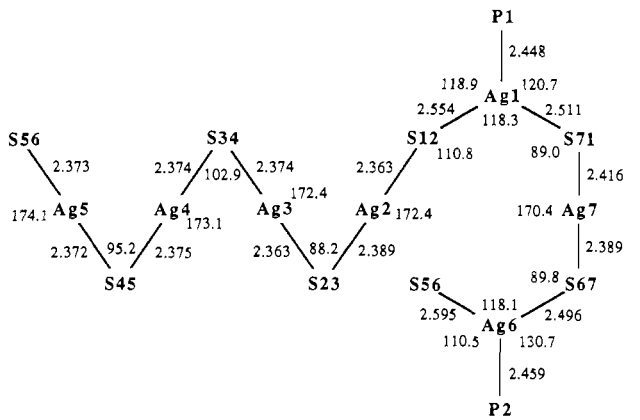

10

Figure 1. Diagrammatic representation of the atom labeling, bond lengths (Å), and bond angles (deg) for **8** and **9** and for the asymmetric unit of **10**. Secondary connections are shown (as shaded lines) for **9** but not **10**.

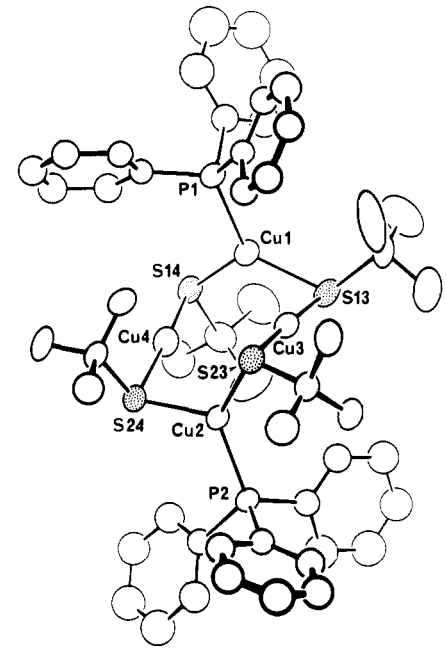

Figure 2. Molecular structure of $(CuSBu^t)_4(Ph_3P)_2$ (**8**).

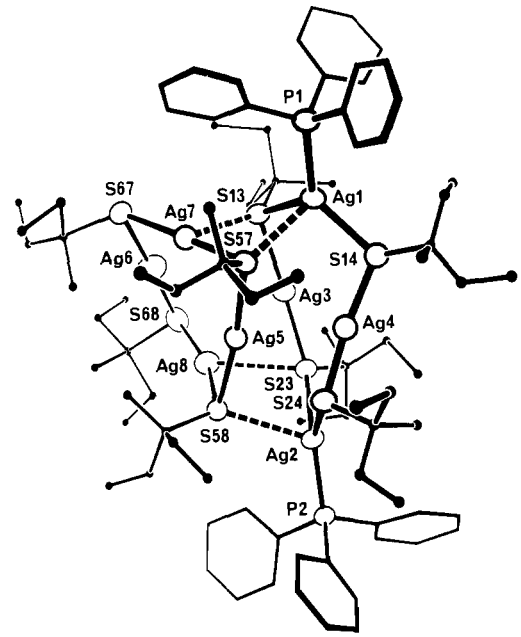

Figure 3. Molecular structure of $(AgSCMeEt_2)_8(PPh_3)_2$ (**9**) with the Ag, S, and P atoms shown as 20% probability ellipsoids and, for clarity, alkyl C atoms as arbitrary small circles and phenyl groups as hexagons. The weak secondary interactions are drawn as broken lines.

be described as an approximation to the chair conformation of a six-membered ring. The chair is distorted, by twisting the two linear segments to a twist-chair conformation and by folding of the Cu^{trig} coordination planes perpendicular to the central section. The coordination planes of the Cu^{trig} atoms are within 4° of being parallel. The two Cu-P bonds and the thiolate substituents at S14 and S24 are "axial" to this chair, while the substituents at S13 and S23 are "equatorial". Consequently the conformations of the thiolate substituents at the ends of the two S–Cu–S linear segments are different: across Cu3 the C–S23–(Cu3)–S13–C torsional angle is −47.1°, whereas C–S24–(Cu4)–S14–C is −173.4°. The reason for this difference is found in the packing of the phenyl and Bu^t substituents over the surface of the molecule. At each $S_2Cu–PPh_3$ moiety one P–C bond virtually eclipses a Cu–S bond, for which the thiolate Bu^t substituent must oppose the phenyl group and consequently be axial to the molecular ring. The thiolate substituents that are equatorial to the ring fit between the other two phenyl substituents of each PPh_3 ligand.

The Cu^{trig}–S bonds are elongated by 0.10 Å relative to the mean Cu^{dig}–S distance of 2.16 [0.01] Å.[16] There is a small but significant steric influence of the Bu^t substituents on the Cu^{dig}–S bond lengths: at Cu4, where the Bu^t substituents at S14 and S24 are opposed (torsional angle −173.4°), the Cu–S distances 2.145 (2) and 2.150 (2) Å are unrestrained, but at Cu3, where the substituents on S13 and S23 are twisted by only −47.1° about the S–Cu–S vector, the distances are elongated to 2.163 (3) and 2.167 (2) Å. The Cu^{trig} atoms Cu1 and Cu2 are only 0.05 and 0.09 Å, respectively, from their best CuS_2P planes (see Table VIII). Angles at Cu^{trig} deviate by up to 10° from 120°, and the usual correlation between each angle θ (deg) and its opposing bond length d (Å),[1] occurs as $d = 2.152 + 8.39 \times 10^{-4}\theta$, with a regression coefficient $r = 0.98$. The Cu–P and Cu–S bonds equally fit this correlation, and there is no distinction between the lengths of Cu–(μ-SBu^t) and $Cu–PPh_3$ bonds.

Structure of 9. This compound contains two different tetrasilver cycles, one ($(\mu$-$SCMeEt)_4Ag_4$) with digonal silver (Ag^{dig}) only,

Table III. Positional Parameters for the Non-Hydrogen Atoms of **9**

atom	x/a	y/b	z/c	atom	x/a	y/b	z/c
Ag1	0.4259 (1)	0.1716 (1)	0.8069 (1)	C43P2	−0.3046 (17)	0.2067 (10)	0.5129 (10)
Ag2	0.0526 (1)	0.2806 (1)	0.6367 (1)	C53P2	−0.3224 (16)	0.2531 (10)	0.5075 (10)
Ag3	0.1865 (1)	0.1607 (1)	0.7499 (1)	C63P2	−0.2617 (15)	0.2868 (8)	0.5343 (9)
Ag4	0.2666 (1)	0.2693 (1)	0.7261 (1)	C113	0.2665 (15)	0.0756 (8)	0.8496 (9)
Ag5	0.2486 (1)	0.1839 (1)	0.6377 (1)	C213	0.1733 (5)	0.0498 (8)	0.8285 (9)
Ag6	0.1766 (1)	0.0285 (1)	0.6797 (1)	C313	0.1354 (23)	0.0263 (13)	0.8808 (15)
Ag7	0.3561 (1)	0.0834 (1)	0.6839 (1)	C413	0.3465 (18)	0.0454 (10)	0.8795 (11)
Ag8	0.0608 (1)	0.1267 (1)	0.6449 (1)	C513	0.3548 (17)	−0.0007 (10)	0.8422 (11)
P1	0.5771 (3)	0.1396 (2)	0.8458 (2)	C613	0.2581 (16)	0.1213 (9)	0.8917 (10)
P2	−0.0972 (3)	0.3161 (2)	0.6006 (2)	C114	0.3936 (15)	0.3001 (8)	0.8489 (9)
S13	0.2987 (3)	0.1021 (2)	0.7864 (2)	C214	0.3125 (16)	0.3349 (9)	0.8545 (10)
S14	0.3286 (3)	0.2454 (2)	0.8168 (2)	C314	0.3495 (23)	0.3808 (13)	0.8886 (14)
S23	0.0605 (3)	0.2115 (2)	0.7133 (2)	C414	0.4545 (17)	0.2832 (9)	0.9013 (11)
S24	0.2168 (3)	0.3056 (2)	0.6386 (2)	C514	0.3968 (18)	0.2602 (10)	0.9410 (11)
S57	0.3993 (3)	0.1687 (2)	0.6862 (2)	C614	0.4548 (15)	0.3227 (8)	0.8101 (10)
S58	0.0983 (3)	0.1908 (2)	0.5843 (2)	C123	−0.0107 (14)	0.2189 (8)	0.7684 (9)
S67	0.3255 (4)	−0.0034 (2)	0.6750 (2)	C223	0.0419 (25)	0.2439 (14)	0.8146 (15)
S68	0.0235 (4)	0.0504 (2)	0.6853 (2)	C323	0.0449 (20)	0.3017 (11)	0.7964 (12)
C11P1	0.6676 (12)	0.1867 (7)	0.8582 (8)	C423	−0.1078 (20)	0.2359 (11)	0.7426 (12)
C21P1	0.6593 (14)	0.2280 (8)	0.8282 (8)	C523	−0.1557 (25)	0.1891 (14)	0.7151 (16)
C31P1	0.7262 (16)	0.2648 (8)	0.8358 (9)	C623	−0.0188 (19)	0.1660 (11)	0.7985 (12)
C41P1	0.7936 (16)	0.2593 (9)	0.8751 (10)	C124	0.2327 (16)	0.3719 (8)	0.6436 (10)
C51P1	0.8070 (15)	0.2191 (9)	0.9056 (9)	C224	0.1829 (25)	0.3917 (14)	0.5893 (15)
C61P1	0.7452 (15)	0.1813 (8)	0.8981 (9)	C324	0.1801 (34)	0.4482 (20)	0.5871 (21)
C12P1	0.6208 (14)	0.0921 (7)	0.8078 (8)	C424	0.3369 (20)	0.3868 (10)	0.6611 (12)
C22P1	0.5593 (14)	0.0563 (8)	0.7830 (9)	C524	0.3658 (31)	0.3827 (16)	0.6078 (19)
C32P1	0.5812 (16)	0.0176 (8)	0.7526 (9)	C624	0.1862 (20)	0.3930 (11)	0.6904 (12)
C42P1	0.6727 (19)	0.0168 (9)	0.7491 (10)	C157	0.4867 (15)	0.1791 (9)	0.6409 (9)
C52P1	0.7373 (17)	0.0496 (10)	0.7728 (10)	C257	0.4819 (24)	0.2326 (14)	0.6224 (15)
C62P1	0.7105 (16)	0.0889 (9)	0.8016 (9)	C357	0.5199 (25)	0.2609 (14)	0.6713 (16)
C13P1	0.5788 (13)	0.1128 (8)	0.9136 (8)	C457	0.4421 (19)	0.1514 (11)	0.5853 (12)
C23P1	0.6110 (17)	0.0672 (10)	0.9279 (11)	C557	0.5176 (28)	0.1305 (15)	0.5574 (17)
C33P1	0.6038 (18)	0.0446 (10)	0.9809 (12)	C657	0.5801 (19)	0.1443 (10)	0.6660 (11)
C43P1	0.5698 (18)	0.0757 (11)	1.0107 (11)	C158	0.1069 (13)	0.1723 (7)	0.5151 (8)
C53P1	0.5353 (17)	0.1204 (10)	1.0030 (11)	C258	0.1699 (19)	0.2067 (11)	0.4886 (11)
C63P1	0.5373 (15)	0.1378 (8)	0.9483 (10)	C358	0.1376 (18)	0.2587 (11)	0.4823 (11)
C11P2	−0.1565 (13	0.3471 (7)	0.6504 (7)	C458	−0.0001 (22)	0.1642 (11)	0.4877 (12)
C21P2	−0.2401 (15)	0.3337 (8)	0.6577 (9)	C558	−0.0130 (37)	0.1389 (20)	0.4461 (22)
C31P2	−0.2828 (18)	0.3585 (10)	0.6987 (12)	C658	0.1553 (16)	0.1214 (9)	0.5157 (10)
C41P2	−0.2297 (18)	0.3949 (9)	0.7281 (10)	C167	0.3316 (18)	−0.0256 (10)	0.6012 (10)
C51P2	−0.1483 (19)	0.4083 (9)	0.7199 (11)	C267	0.4487 (26)	−0.0235 (13)	0.6022 (15)
C61P2	−0.1076 (14)	0.3847 (8)	0.6797 (9)	C367	0.4450 (43)	−0.0307 (23)	0.5395 (28)
C12P2	−0.0922 (14)	0.3622 (7)	0.5483 (8)	C467	0.2580 (27)	−0.0707 (16)	0.5882 (16)
C22P2	−0.0347 (15)	0.3506 (9)	0.5143 (10)	C567	0.3086 (32)	−0.1015 (17)	0.6141 (20)
C32P2	−0.0268 (18)	0.3858 (11)	0.4705 (11)	C667	0.2854 (19)	0.0152 (11)	0.5633 (12)
C42P2	−0.0787 (19)	0.4274 (10)	0.4655 (11)	C168	−0.0567 (15)	0.0151 (8)	0.6353 (9)
C52P2	−0.1346 (18)	0.4373 (10)	0.5002 (12)	C268	−0.1447 (22)	0.0491 (12)	0.6296 (13)
C62P2	−0.1462 (16)	0.4024 (9)	0.5415 (10)	C368	−0.2157 (30)	0.0299 (16)	0.5994 (18)
C13P2	−0.1801 (12)	0.2736 (7)	0.5672 (7)	C468	−0.0537 (16)	−0.0396 (9)	0.6513 (11)
C23P2	−0.1642 (14)	0.2238 (8)	0.5719 (8)	C568	−0.0859 (19)	−0.0447 (10)	0.7057 (12)
C33P2	−0.2276 (18)	0.1884 (9)	0.5445 (10)	C668	−0.0197 (16)	0.0147 (9)	0.5785 (10)

and the other ($(\mu$-$SCMeEt_2)_4Ag_2(AgPPh_3)_2$) with two Ag^{dig} atoms and two opposite Ag^{trig} metal atoms, Ag1 and Ag2, each with a Ph_3P ligand. The structure is shown in Figure 3. The $((Ag^{dig})_2(Ag^{trig})_2)$ cycle has the same connectivity as **8**, but a distinctly different, elongated, conformation in which the Ag^{trig} planes are approximately coplanar with the other Ag and S atoms.

The two cycles are associated and linked by four long secondary connections that are drawn as broken lines on Figure 3. The differentiation of primary and secondary coordination of silver by thiolate in this structure is unequivocal, being based on the interatomic distances and on the minor perturbations from digonal or trigonal coordination stereochemistry. There are 12 primary Ag^{dig}–S bonds, those at Ag3 to Ag8, with a mean value of 2.39 [2] Å.[16] The secondary intercycle connections at the digonal silver atoms Ag7 and Ag8 are 2.86 and 2.87 Å, almost 0.5 Å longer than the primary bonds. At the trigonal silver atoms Ag1 and Ag2 the primary Ag^{trig}–S bonds range from 2.50 to 2.66 Å, and the secondary connections, 2.90 and 2.97 Å, are ca. 0.4 Å longer. The best evidence for the weakness of the secondary bonding appears in the minor angular perturbations of the primary bonding: the S–Ag^{dig}–S angles are 173.5 and 165.7° at Ag7 and Ag8, respectively, compared with a mean value of 173° at the other uninvolved Ag^{dig} atoms; the trigonal Ag2 is displaced only 0.15 Å from its coordination plane by its secondary connection while at Ag1 the out-of-plane displacement toward S57 is 0.28 Å (see Figure 3 and Table VIII).

On each of the two cycles the tertiary thiolate substituents are syn, and directed away from the other cycle. The thiolate substituents effectively enclose the Ag,S cycles, while the phenyl rings of the phosphine ligands protrude beyond the molecular surface created by the thiolate substituents.

Both cycles are slightly twisted from planarity. In the $(Ag^{dig})_4$ cycle the Ag–S–Ag angles range from 78 to 86°, while in the $(Ag^{dig})_2(Ag^{trig})_2$ cycle the angles at S are larger and more variable, and the S–Ag^{trig}–S angles (101, 105°) are substantially less than 120°. Within the primary trigonal coordination planes, variations in the Ag^{trig}–S and Ag^{trig}–P distances correlate with deviations from 120° in the opposite angles.

Structure of 10. This molecule, shown in Figure 4, is (μ-$SBu^t)_{14}Ag_{10}(AgPPh_3)_4$. It is a single 28-membered cycle of alternating silver and sulfur atoms, with 10 linear S–Ag^{dig}–S segments and four angular segments in which phosphine ligands are

(16) Standard deviations reported in brackets are those of the *sample*, not the mean.

Table IV. Positional Parameters for the Non-Hydrogen Atoms of **10**

atom	x/a	y/b	z/c	atom	x/a	y/b	z/c
Ag1	0.2351 (2)	0.5946 (2)	0.7597 (1)	C371	0.4029 (37)	0.5270 (35)	0.9595 (23)
Ag2	0.3666 (2)	0.3624 (2)	0.6891 (1)	C471	0.2996 (32)	0.6752 (32)	0.9258 (19)
Ag3	0.5679 (2)	0.3939 (2)	0.5946 (1)	C11P1	0.0257 (19)	0.6985 (21)	0.8413 (12)
Ag4	0.6105 (2)	0.4495 (2)	0.4224 (1)	C21P1	0.0108 (23)	0.7698 (23)	0.8774 (16)
Ag5	0.4824 (2)	0.4952 (2)	0.2847 (1)	C31P1	−0.0431 (27)	0.7437 (28)	0.9374 (17)
Ag6	0.4295 (2)	0.7783 (2)	0.2005 (1)	C41P1	−0.0723 (26)	0.6489 (30)	0.9586 (16)
Ag7	0.6151 (2)	0.6038 (2)	0.1735 (1)	C51P1	−0.0595 (23)	0.5860 (23)	0.9199 (16)
S12	0.2178 (6)	0.4626 (6)	0.6934 (4)	C61P1	−0.0115 (22)	0.6033 (22)	0.8600 (14)
S23	0.5132 (6)	0.2622 (5)	0.6705 (3)	C12P1	0.1361 (22)	0.8404 (20)	0.7618 (12)
S34	0.6390 (5)	0.5111 (5)	0.5142 (3)	C22P1	0.0772 (24)	0.9265 (26)	0.7402 (14)
S45	0.5970 (6)	0.3732 (5)	0.3343 (4)	C32P1	0.1077 (28)	1.0229 (26)	0.7419 (16)
S56	0.3553 (6)	0.6104 (6)	0.2428 (4)	C42P1	0.1957 (30)	1.0320 (26)	0.7647 (17)
S67	0.6086 (6)	0.7785 (6)	0.1641 (4)	C52P1	0.2567 (27)	0.9499 (29)	0.7860 (16)
S71	0.3694 (6)	0.5680 (6)	0.8360 (4)	C62P1	0.2266 (28)	0.8517 (27)	0.7829 (16)
P1	0.0972 (6)	0.7173 (6)	0.7679 (4)	C13P1	0.0028 (22)	0.7285 (19)	0.7093 (14)
P2	0.2976 (6)	0.9113 (6)	0.1901 (4)	C23P1	0.0349 (24)	0.7183 (22)	0.6491 (17)
C112	0.1167 (21)	0.3836 (20)	0.7229 (14)	C33P1	−0.0317 (27)	0.7233 (22)	0.6030 (15)
C212	0.1273 (23)	0.2872 (22)	0.6937 (14)	C43P1	−0.1296 (25)	0.7422 (22)	0.6181 (15)
C312	0.0199 (26)	0.4446 (25)	0.7020 (16)	C53P1	−0.1660 (23)	0.7542 (21)	0.6784 (16)
C412	0.1099 (24)	0.3583 (23)	0.7918 (16)	C63P1	−0.0998 (23)	0.7473 (20)	0.7260 (14)
C123	0.4756 (22)	0.1664 (21)	0.6275 (14)	C11P2	0.2235 (20)	0.9080 (21)	0.2619 (13)
C223	0.4107 (25)	0.2106 (24)	0.5762 (16)	C21P2	0.2033 (22)	0.9909 (22)	0.2924 (15)
C323	0.5718 (33)	0.1243 (31)	0.5991 (20)	C31P2	0.1522 (23)	0.9805 (23)	0.3507 (15)
C423	0.4159 (28)	0.0906 (27)	0.6718 (18)	C41P2	0.1174 (23)	0.8889 (26)	0.3782 (15)
C134	0.7778 (23)	0.4870 (23)	0.5263 (15)	C51P2	0.1373 (24)	0.8076 (23)	0.3498 (16)
C234	0.8209 (27)	0.5842 (26)	0.4802 (17)	C61P2	0.1905 (23)	0.8155 (22)	0.2941 (15)
C334	0.8146 (25)	0.3949 (26)	0.5066 (16)	C12P2	0.3364 (22)	1.0375 (19)	0.1721 (12)
C434	0.7935 (24)	0.4916 (23)	0.5922 (16)	C22P2	0.2653 (23)	1.1180 (23)	0.1439 (14)
C145	0.5248 (23)	0.2588 (21)	0.3565 (14)	C32P2	0.3004 (28)	1.2172 (25)	0.1301 (15)
C245	0.5070 (23)	0.2189 (23)	0.2993 (15)	C42P2	0.3941 (28)	1.2288 (24)	0.1426 (15)
C345	0.5989 (28)	0.1846 (27)	0.3999 (17)	C52P2	0.4653 (22)	1.1514 (24)	0.1632 (14)
C445	0.4342 (24)	0.2762 (22)	0.3975 (15)	C62P2	0.4315 (23)	1.0564 (22)	0.1772 (13)
C156	0.2953 (23)	0.5573 (22)	0.1876 (15)	C13P2	0.2046 (26)	0.9066 (22)	0.1308 (16)
C256	0.1977 (26)	0.6266 (25)	0.1632 (16)	C23P2	0.1004 (32)	0.9170 (27)	0.1516 (18)
C356	0.3573 (36)	0.5381 (33)	0.1316 (22)	C33P2	0.0310 (35)	0.9183 (30)	0.0991 (24)
C456	0.2589 (29)	0.4562 (30)	0.2182 (18)	C43P2	0.0759 (36)	0.8987 (29)	0.0461 (21)
C167	0.6227 (26)	0.8311 (25)	0.0784 (15)	C53P2	0.1733 (43)	0.8921 (34)	0.0290 (23)
C267	0.7344 (31)	0.8063 (27)	0.0588 (18)	C63P2	0.2443 (29)	0.8944 (27)	0.0747 (21)
C367	0.5527 (31)	0.7871 (29)	0.0399 (19)	Cl1	0.2744 (9)	0.0229 (8)	0.4942 (6)
C467	0.6000 (28)	0.9417 (28)	0.0719 (17)	Cl2	0.1423 (9)	0.1413 (9)	0.5597 (6)
C171	0.3215 (25)	0.5706 (23)	0.9143 (14)	Cl3	0.1073 (11)	−0.0584 (11)	0.5613 (7)
C271	0.2312 (29)	0.5236 (27)	0.9347 (17)	C	0.1897 (32)	0.0206 (32)	0.5657 (19)

Table V. Bond Lengths (Å) and Angles (deg) for **8**

Cu1–S13	2.247 (2)	Cu2–S23	2.245 (2)
Cu1–S14	2.263 (2)	Cu2–S24	2.260 (2)
Cu1–P1	2.253 (2)	Cu2–P2	2.249 (2)
Cu3–S13	2.163 (3)	Cu4–S14	2.150 (2)
Cu3–S23	2.167 (2)	Cu4–S24	2.145 (2)
S13–Cu1–P1	130.5 (1)	S23–Cu2–P2	129.7 (1)
S14–Cu1–P1	110.6 (1)	S24–Cu2–P2	112.8 (1)
S13–Cu1–S14	118.6 (1)	S23–Cu2–S24	116.6 (1)
S13–Cu3–S23	176.0 (1)	S14–Cu4–S24	172.6 (1)
Cu1–S13–Cu3	80.5 (1)	Cu2–S23–Cu3	79.9 (1)
Cu1–S13–C113	119.2 (3)	Cu2–S23–C123	116.6 (2)
Cu3–S13–C113	106.3 (3)	Cu3–S23–C123	107.8 (3)
Cu1–S14–Cu4	84.5 (1)	Cu2–S24–Cu4	89.9 (1)
Cu1–S14–C114	114.9 (3)	Cu2–S24–C124	113.4 (2)
Cu4–S14–C114	104.5 (3)	Cu4–S24–C124	105.1 (2)
Cu1–P1–C11P1	110.4 (3)	Cu2–P2–C11P2	108.2 (2)
Cu1–P1–C12P1	117.5 (2)	Cu2–P2–C12P2	115.7 (3)
Cu1–P1–C13P1	115.8 (2)	Cu2–P2–C13P2	119.5 (3)
C11P1–P1–C12P1	103.5 (4)	C11P2–P2–C12P2	102.9 (4)
C11P1–P1–C13P1	104.2 (4)	C11P2–P2–C13P2	106.3 (4)
C12P1–P1–C13P1	103.9 (3)	C12P2–P2–C13P2	102.7 (4)

attached to create trigonal-planar coordination of Ag^{trig}. It is the largest such cycle known. In addition to the actual center of symmetry, there is a pseudo-2-fold axis along the length of the molecule, Ag7---Ag7′, relating *all atoms* except the Ph_3P phenyl rings. As shown in Figure 4a, the ligand substituents effectively enclose the Ag and S atoms. This enclosure is in the form of a rectangular box, in which four of the six faces are created by the thiolate substituents, while the phosphine ligands protrude through the other two faces of the molecular box. The chloroform in the lattice is located between the pairs of PPh_3 ligands protruding on the same side of the box.

We analyze and discuss this molecular structure in terms of its component S–Ag–S segments, shown in Figure 5 as a diagrammatic representation of Figure 4a. Two pairs of linear S–Ag–S segments in the front and back faces of the box form opposing *zigzag* sections that are linked to four linear segments which *cross over* the top and bottom faces of the box, and then the chain continues to wrap around the box through four *bending* (trigonal) segments over the front and back faces. The cycle is completed by two linear *end-connecting* segments in the end faces of the box. Evidently the bending section is required to connect the crossover and end sections without the Ag–S–Ag angles becoming too acute. Features of the structures of **2** and **9** are combined in **10**. Each end of **10**, formed by an end segment and two bending segments, is comparable with the $S–Ag^{trig}–S–Ag^{dig}–S–Ag^{trig}–S$ sequence in the $(Ag^{dig})_2(Ag^{trig})_2$ cycle of **9**. The zigzag and crossover segments of **10** correspond closely with segments of the same type in the extended chain structure of **2**.

Mean values of comparable dimensions are as follows: $Ag^{dig}–S$, 2.38 [2] Å;[16] $Ag^{trig}–S$, 2.54 [4] Å; $S–Ag^{dig}–S$ 173 [1]°. In this molecule there are only four secondary Ag---S interactions, one at each trigonal Ag atom, namely Ag1---S45′ = 2.96 Å, Ag6---S23′ = 2.92 Å, and the symmetry-related pair. The minimal bonding significance of these secondary interactions is revealed by their negligible perturbation of the trigonal stereochemistry at Ag1 and Ag6, for which the out-of-plane displacements are 0.16 and 0.08 Å respectively (Table VIII). The more significant feature of the structure is one found also in **2**, namely an arrangement of the segments such that four relatively close contracycle Ag to Ag contacts occur across the molecular axis:

Table VI. Bond Lengths (Å) and Angles (deg) for **9**

Ag1–S13	2.644 (5)	Ag2–S23	2.662 (5)
Ag1–S14	2.498 (6)	Ag2–S24	2.507 (5)
Ag1–P1	2.434 (5)	Ag2–P2	2.435 (5)
Ag3–S13	2.362 (5)	Ag4–S14	2.380 (6)
Ag3–S23	2.366 (5)	Ag4–S24	2.392 (6)
Ag5–S57	2.377 (5)	Ag6–S67	2.381 (6)
Ag5–S58	2.388 (5)	Ag6–S68	2.361 (6)
Ag7–S57	2.397 (5)	Ag8–S58	2.427 (5)
Ag7–S67	2.400 (6)	Ag8–S68	2.405 (6)
Ag1---S57	2.967 (5)	Ag2---S58	2.897 (5)
Ag7---S13	2.872 (5)	Ag8---S23	2.863 (5)
S13–Ag1–P1	113.1 (2)	S23–Ag2–P2	118.0 (2)
S14–Ag1–P1	138.4 (2)	S24–Ag2–P2	135.3 (2)
S13–Ag1–S14	100.9 (2)	S23–Ag2–S24	104.7 (2)
S13–Ag3–S23	172.8 (2)	S14–Ag4–S24	170.8 (2)
S57–Ag5–S58	173.8 (2)	S67–Ag6–S68	173.2 (2)
S57–Ag7–S67	173.5 (2)	S58–Ag8–S68	165.7 (2)
Ag1–S13–Ag3	91.2 (2)	Ag2–S23–Ag3	128.4 (2)
Ag1–S13–C113	112.7 (7)	Ag2–S23–C123	119.3 (7)
Ag3–S13–C113	108.8 (7)	Ag3–S23–C123	106.2 (7)
Ag1–S14–Ag4	105.0 (2)	Ag2–S24–Ag4	92.8 (2)
Ag1–S14–C114	114.7 (7)	Ag2–S24–C124	112.5 (8)
Ag4–S14–C114	106.1 (7)	Ag4–S24–C124	109.2 (8)
Ag5–S57–Ag7	86.2 (2)	Ag6–S67–Ag7	78.4 (2)
Ag5–S57–C157	110.2 (8)	Ag6–S67–C167	110.5 (8)
Ag7–S57–C157	109.7 (7)	Ag7–S67–C167	110.6 (8)
Ag5–S58–Ag8	83.4 (2)	Ag6–S68–Ag8	84.4 (2)
Ag5–S58–C158	107.4 (6)	Ag6–S68–C168	109.8 (7)
Ag8–S58–C158	116.9 (7)	Ag8–S68–C168	109.3 (7)
Ag1–P1–C11P1	114.1 (6)	Ag2–P2–C11P2	115.9 (6)
Ag1–P1–C12P1	115.7 (7)	Ag2–P2–C12P2	113.1 (7)
Ag1–P1–C13P1	112.1 (7)	Ag2–P2–C13P2	115.0 (6)
C11P1–P1–C12P1	105.9 (9)	C11P2–P2–C12P2	104.7 (9)
C11P1–P1–C13P1	103.0 (9)	C11P2–P2–C13P2	104.2 (8)
C12P1–P1–C13P1	104.8 (9)	C12P2–P2–C13P2	102.6 (8)

Table VII. Bond Lengths (Å) and Angles (deg) for **10**[a]

Ag1–S12	2.554 (8)	Ag4–S45	2.375 (8)
Ag1–S71	2.511 (9)	Ag5–S45	2.372 (8)
Ag2–S12	2.363 (8)	Ag5–S56	2.373 (8)
Ag2–S23	2.389 (8)	Ag6–S56	2.595 (8)
Ag3–S23	2.363 (8)	Ag6–S67	2.496 (9)
Ag3–S34	2.374 (8)	Ag7–S67	2.389 (9)
Ag4–S34	2.374 (8)	Ag7–S71^{i}	2.416 (9)
Ag1–P1	2.448 (8)	Ag6–P2	2.459 (8)
Ag1---S45^{i}	2.96 (1)	Ag6---S23^{i}	2.92 (1)
S12–Ag1–S71	118.3 (3)	S45–Ag5–S56	174.1 (3)
S12–Ag1–P1	118.9 (3)	S56–Ag6–S67	118.1 (3)
S71–Ag1–P1	120.7 (3)	S56–Ag6–P2	110.5 (3)
S12–Ag2–S23	172.4 (3)	S67–Ag6–P2	130.7 (3)
S23–Ag3–S34	172.4 (3)	S67–Ag7–S71^{i}	170.1 (3)
S34–Ag4–S45	173.1 (3)		
Ag1–S12–Ag2	110.8 (3)	Ag5–S45–C145	105 (1)
Ag1–S12–C112	113 (1)	Ag5–S56–Ag6	109.6 (3)
Ag2–S12–C112	108 (1)	Ag5–S56–C156	108 (1)
Ag2–S23–Ag3	88.2 (3)	Ag6–S56–C156	116 (1)
Ag2–S23–C123	107 (1)	Ag6–S67–Ag7	89.8 (3)
Ag3–S23–C123	107 (1)	Ag6–S67–C167	111 (1)
Ag3–S34–Ag4	102.9 (3)	Ag7–S67–C167	107 (1)
Ag3–S34–C134	102 (1)	Ag7^{i}–S71–Ag1	89.0 (3)
Ag4–S34–C134	106 (1)	Ag7^{i}–S71–C171	105 (1)
Ag4–S45–Ag5	95.2 (3)	Ag1–S71–C171	112 (1)
Ag4–S45–C145	111 (1)		
Ag1–P1–C11P1	114 (1)	Ag6–P2–C11P2	111 (1)
Ag1–P1–C12P1	114 (1)	Ag6–P2–C12P2	117 (1)
Ag1–P1–C13P1	116 (1)	Ag6–P2–C13P2	116 (1)
C11P1–P1–C12P1	103 (1)	C11P2–P2–C12P2	104 (1)
C11P1–P1–C13P1	104 (1)	C11P2–P2–C13P2	104 (1)
C12P1–P1–C13P1	104 (1)	C12P2–P2–C13P2	104 (1)

[a] Key: (i) $1-x, 1-y, 1-z$.

Ag3---Ag4′ = 3.12 (1) Å; Ag2---Ag5′ = 3.09 (1) Å. These are nonbonding distances for two-coordinate silver. Two other contracycle distances between Ag atoms in the bend and end segments are Ag2---Ag7′ = 3.14 (1) Å and Ag5---Ag7 = 3.14 (1) Å. In

Table VIII. Displacements (Å) of Trigonal Metal Atoms from Their Coordination Planes[a]

			Compound **8**				
Cu1	−0.05	S13	0.02	S14	0.02	P1	0.02
Cu2	−0.09	S23	0.03	S24	0.03	P2	0.03
			Compound **9**				
Ag1	−0.28	S13	0.07	S14	0.10	P1	0.11
Ag2	−0.15	S23	0.04	S24	0.05	P2	0.06
			Compound **10**				
Ag1	−0.16	S12	0.05	S71	0.05	P1	0.05
Ag6	−0.08	S56	0.02	S67	0.03	P2	0.03

[a] All four atoms were included in the calcualtion of the least-squares plane.

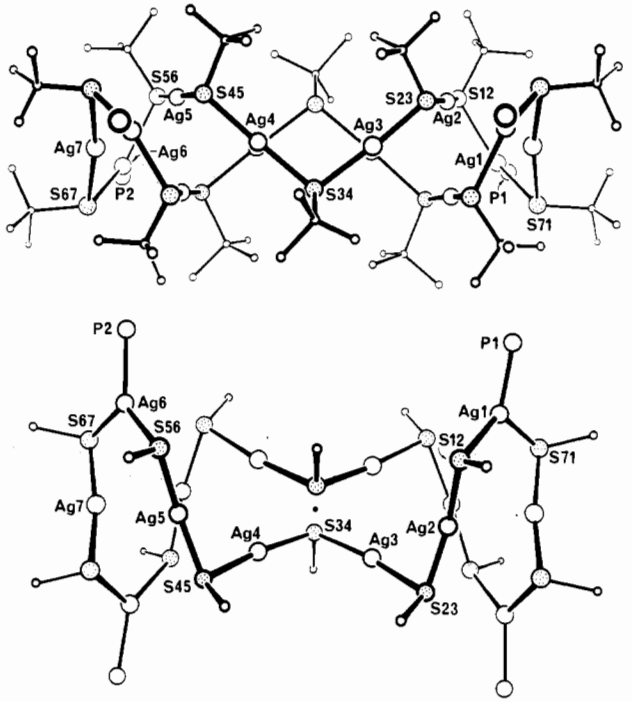

Figure 4. Two views of the centrosymmetric molecule $(\mu\text{-SBu}^t)_{14}Ag_{10}(AgPPh_3)_4$ (**10**). Carbon atoms are drawn as arbitrary small circles, for clarity. (a, top) View with all atoms except those of the phenyl groups, showing the zigzag, crossover, and end segments and the boxlike molecular shape. (b, bottom) View after rotation of the molecule from part a by 70° about the pseudo-2-fold axis Ag7---Ag7′, including only the thiolate Cα atoms.

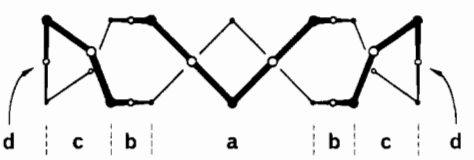

Figure 5. Diagrammatic representation of the structural sections of **10**: (a) zigzag; (b) crossover; (c) bending; (d) end-connecting. The view direction is comparable with that of Figure 4a.

10, as in **2**, the Ag–S–Ag angle between zigzag segments, 102.9°, is larger than that between zigzag and crossover segments (88.2, 95.2°).

Structural Principles. We are now able to examine details of seven related but different types of structure for copper and silver compounds with tertiary alkanethiolate or bulky secondary alkanethiolate ligands: $[AgSCMeEt_2]_\infty$ (**2**); $[AgSC(SiMe_3)_3]_4$ (**3**);

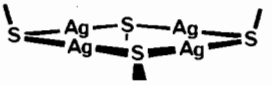

3

$[AgSCH(SiMe_3)_2]_8$ (**5**); $(CuSBu^t)_4(Ph_3P)_2$ (**8**); $(AgSCMeEt_2)_8(Ph_3P)_2$ (**9**); $(AgSBu^t)_{14}(Ph_3P)_4$ (**10**): $[M_5(SBu^t)_6]^-$

(**11**; M = Cu, Ag[17]). All of these structures, including **2**, which

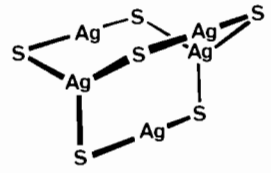

11

is one-dimensionally nonmolecular, are effectively insulated from their crystalline environments by ligand substituents.

Clearly defined structural moieties recur: (a) In all structures there occur doubly bridging thiolates, chains of alternating M and S atoms, and linear $-(\mu\text{-SR})-M-(\mu\text{-SR})-$ segments. (b) Trigonal $(\mu\text{-SR})_2M(PPh_3)$ segments occur in **8**–**10**, and trigonal $(\mu\text{-SR})_3M$ segments occur in **11**. (c) Linear segments form coplanar zigzag sequences, with two segments per sequence in **10** and three segments per sequence in **2**. (d) Approximately parallel planes of zigzag sequences occur in opposite faces of **2** and **10**, with the closest contacts between opposing segments being M---M, but at nonbonding distances. The central section of **8** is similarly composed of two opposing linear segments. (e) $(\mu\text{-SR})_4M_4$ cycles occur in **3**, **5**, **9**, and **11**, while related $(\mu\text{-SR})_4M_4(PPh_3)_2$ cycles occur in **8**, and **9** (and, almost, in **10**; see below).

The number density of substituents along a –M–SR–M–SR– sequence is not high, and even tertiary alkyl substituents cannot enclose a single $-(M-SR)_n-$ strand. In all except **2** the strands form cycles, and in all structures except **3**, which has the bulkiest substituents, some mode of agglomeration occurs in order to increase the density of substituents on the molecular surface. One structural agglomeration mode, in **5** and **9**, is confacial association of Ag_4 cycles, supported by secondary M---S interactions. Another agglomeration mode, most clearly evident in the structures of **2** and **10**, involves folding of large cycles (**10**) or intertwining of strands (**2**) with no (or few) secondary interactions between them. Both of these modes effectively double the density of substituents over the molecular surface. The Ph_3P ligands, which are incorporated at a relatively small proportion of the metal atoms even though they were available in excess in the crystallization solution for **8**–**10**, protrude through the molecular surface and do not appear to have any steric influence on the molecular size or composition of the core.

The recurrence of tetrametallic cycles $(\mu\text{-SR})_4M_4$ is probably a reflection of the acceptable bond angles of 180° at M and approximately 90° at S. In **3**, with the very bulky $C(SiMe_3)_3$ substituents, the M_4S_4 atoms of the cycle are virtually coplanar, and the substituents at the pyramidal S atoms are disposed alternately on either side of the plane. In **9** and **5**, both with substituents of intermediate bulk, the $(\mu\text{-SR})_4M_4$ cycles are folded about an S---S diagonal as illustrated in Figure 6a. It is apparent that the $(\mu\text{-SR})_4M_4$ cycle as a structural unit is relatively floppy, which is not surprising in view of its minimal connectivity. The *cyclo*hexyl substituents of $(AgSC_6H_{11})_{12}$ (**1**) are less demanding, allowing a sprawling larger cycle with intracycle and intercycle secondary interactions in the crystal.

The agglomeration of $(\mu\text{-SR})_4M_4$ cycles in **5** is different from that in **9** and is shown diagrammatically in Figure 6b. The characteristic of **5** is a dihedral angle of 78° between the wings (each comprised of S–Ag–S–Ag–S) of the butterfly. Consequently, the array of eight Ag atoms is close to cubic, and when the distinction between primary and secondary bonding is disregarded, four of the SR groups quadruply bridge four of the cube faces and the other four SR groups are edge bridges.

The structure of the ions $[M_5(\mu\text{-SBu}^t)_6]^-$ (**11**), which have a similar surface density of substituents, is also a derivative of the $(\mu\text{-SR})_4M_4$ cycle as shown in Figure 6c. The cycle is folded about an Ag---Ag diagonal, and an additional $(\mu\text{-SR})-M-(\mu\text{-SR})$ segment is added, creating another $(\mu\text{-SR})_4M_4$ cycle.

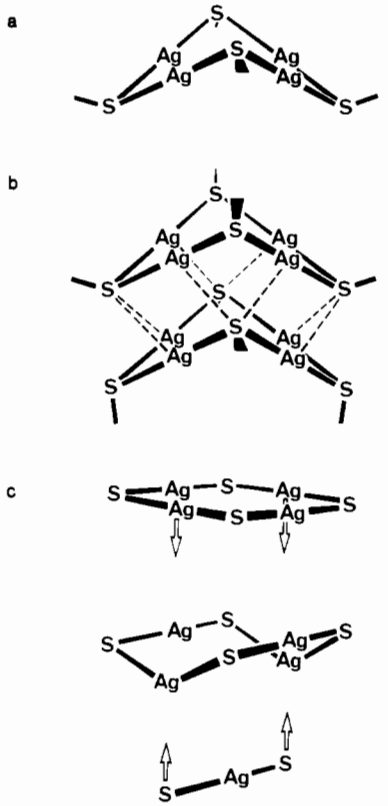

Figure 6. Idealizations of cyclic components of silver thiolate aggregates: (a, top) the folded $(\mu\text{-SR})_4Ag_4$ cycle; (b, middle) association of folded cycles in **5**, to form a pseudocubic Ag_8 array; (c, bottom) the alternative folding of an $(\mu\text{-SR})_4Ag_4$ cycle and association with a linear segment to form **11**.

It has already been mentioned that each end of the molecule of **10** is similar to the $(\mu\text{-SR})_4M_4(PPh_3)_2$ cycle that occurs in **9**. In fact there is a close correspondence between the structures of **9** and **10**, which is best illustrated by the transformation of **9**, which yields **10**, shown in Scheme I. Relatively minor bond rearrangement in the Ag1–S57–Ag7–S13 cycle of **9**, shortening Ag1–S57 and Ag7–S13 to primary bonds and breaking Ag1–S13 and Ag7–S57, creates the single $Ag_8(SR)_8(PPh_3)_2$ cycle (**12**). With minor atom repositioning (and unchanged connectivity), this becomes **13**, which is equivalent to one end of **10** with a connecting atom. The intracycle secondary interactions of **10** do not correspond to secondary or primary bonds in **9** and are a consequence of the Ag7⟹⟸Ag7′ compression of the ends of **10** caused by the crossover and bending segments.

Discussion

The compounds and structures discussed above have analogues in other systems. Copper(I) *tert*-butoxide is a planar tetrametallic molecule, $[(Cu^{dig})_4(\mu\text{-OBu}^t)_4]$, analogous to **3**, but with less pyramidal stereochemistry at the O atoms and hence more equatorially directed substituents.[18] The same planar structure occurs in $[(Cu^{dig})_4(\mu\text{-CH}_2SiMe_3)_4]$[19,20] and in $[(Cu^{dig})_4(\mu\text{-PBu}^t_2)_4]$,[21] while in $[(Cu^{dig})_4(\mu\text{-NEt}_2)_4]$,[22] the cycle is nonplanar. Similar arylcopper and arylsilver compounds are known, with planar cycles and doubly bridging aryl ligands: $[(Cu^{dig})_5(\mu\text{-C}_6H_2Me_3\text{-}2,4,6)_5]$, a pentagonal slightly puckered star with C–Cu–C angles of 146–158°, reacts with tetrahydrothiophene to form $[(\mu\text{-C}_6H_2Me_3\text{-}2,4,6)_4(Cu^{dig})_2(Cu^{trig}SC_4H_8)_2]$.[23] The approximately square $[(Ag^{dig})_4(\mu\text{-}$

(17) (a) Dance, I. G. *J. Chem. Soc., Chem. Commun.* **1976**, 68. (b) Bowmaker, G. A.; Clark, G. R.; Seadon, J. K.; Dance, I. G. *Polyhedron* **1984**, *3*, 535.

(18) Greiser, T.; Weiss, E. *Chem. Ber.* **1976**, *109*, 3142.
(19) Lappert, M. F.; Pearce, R. *J. Chem. Soc., Chem. Commun.* **1973**, 24.
(20) Jarvis, J. A. J.; Kilbourn, B. T.; Pearce, R.; Lappert, M. F. *J. Chem. Soc., Chem. Commun.* **1973**, 475.
(21) Cowley, A. H.; Giolando, D. M.; Jones, R. A.; Nunn, C. M.; Power, J. M. *J. Chem. Soc., Chem. Commun.* **1988**, 208.
(22) Hope, H.; Power, P. P. *Inorg. Chem.* **1984**, *23*, 936.
(23) Gambarotta, S.; Floriani, C.; Chiesi-Villa, A.; Guastini, C. *J. Chem. Soc., Chem. Commun.* **1983**, 1156.

Scheme I. Relationship between the Structures of **9** and **10**, Shown as a Rearrangement Involving Intermediates **12** and **13** and Requiring Only Two Primary Bonds To Be Broken[a]

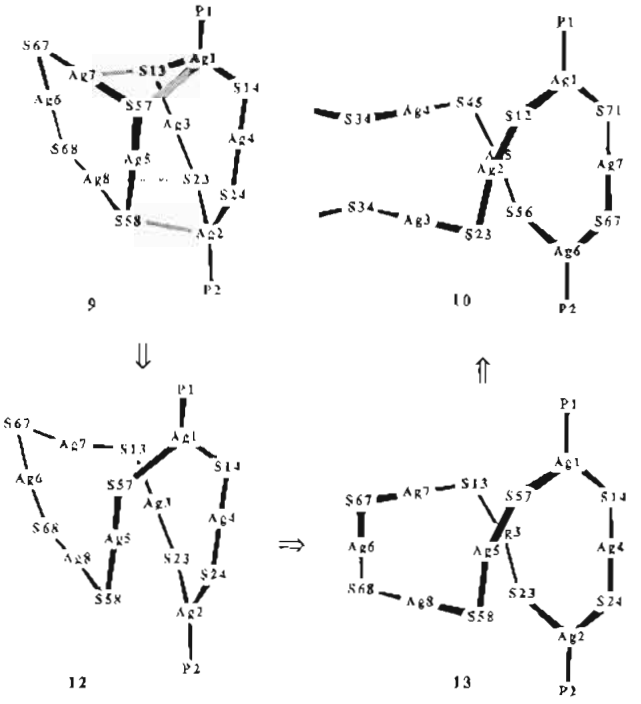

[a] Secondary interactions are shaded. The atom labeling changes between **13** and **10**.

$C_6H_2Me_3$-2,4,6)$_4$] cycle has also been described.[24] The compound $(CuSBu^t)_4(PHBu^t_2)_2$, analogous to **8**, has recently been mentioned, but details are not yet available.[2f] A $[(Cu^{tri8})_4(\mu\text{-}SCMe_2Et)_4]$ cycle occurs in $Cu_4(SCMe_2Et)_4(dppm)_2$.[25]

We summarize as follows the structural principles derived from the results of this paper for copper(I) and silver(I) thiolate complexes with *branched alkyl* substituents: (1) The metal atoms are usually satisfied with linear 2-fold coordination, but may expand to trigonal coordination. (2) Chains of linear segments associate in order to maximize the density of substituents over the M,S core. (3) The minimal number density of M–S bonds in these compounds and the variability of M–S–M angles allow substituent packing to determine conformational details. (4) Segmented chains can be cyclic or extended. (5) Except where the substituents are extremely bulky, the cycles either fold upon themselves or associate confacially in order to maximize the surface density of substituents. (6) Association involves a small number of secondary M---S interactions, which are weak because the metal atoms are coordinatively saturated. (7) Extended segmented chains, from either a folded cycle or intertwined nonmolecular strands, associate with noncentric opposition of segments and M atoms closest, not due to M---M bonding but in order to maximize the separation of SR ligands. (8) The minimal number density of M–S bonds, coupled with secondary S---M interactions, allow facile mechanisms for interchange of structure types, especially interchanges occurring between molecules in solution and nonmolecular crystal structures.

These principles allow another structure type that has not yet been observed. Structure **14**, which can be generalized for any composition $[(MSR)_{2n}(PR_3)_2]$, combines features of **3**, **8**, **9**, and **10**. It differs from **10** in using only zigzag and bending segments

14

and has the trigonal bending segments on the axis of the elongated cycle. The geometry of **14** is satisfactory: taking representative values of Ag^{trig}–S as 2.5 Å, Ag^{dig}–S as 2.38 Å, and S–Ag^{trig}–S as 120°, the angle Ag^{dig}–S–Ag^{dig} calculates as 98°, in good agreement with the values of 100–105° observed in **2** and **10**. Structures **9**, **12**, (or **13**), or **14** could be adopted for molecules $(AgSR)_8(PR_3)_2$ in solution.

Two other models for the structures of compounds $[MSR]_n$ have been derived from the structure of $Cu_8(SCMe_2Et)_4(S_2CSCMe_2Et)_4$.[8] One model, for a nonmolecular structure, has two intertwined helical chains of linked (μ-SR)–M–(μ-SR) segments that are contained in the faces of a square tube. The other, with a simple geometrical relationship to the first, has $(\mu\text{-SR})_4M_4$ cycles encircling the tube and stacked along it. Both structures can have secondary interactions along the tube.

It must be emphasised that the structural principles espoused here are not applicable to analogous copper and silver *arene*thiolate compounds terminated with phosphine ligands, which have clearly different structures.[1,9] Compounds $[AgSAr]_n$ have diffraction patterns characteristic of layered structures, and we will publish separately a postulated structure for such compounds, which have not yet been grown as crystals suitable for full diffraction analysis.[26]

Åkerström has determined that silver tertiary alkanethiolates are octameric $(AgSR^t)_8$ in inert solvents.[2] Among the various structures observed in crystals, cyclic $(AgSR^t)_8$ does not appear as such. On the basis of the observed crystal structures, the best proposal for the octamer would be a pair of associated tetramers, as in **5**. However it is quite conceivable, and probably more likely, that a single $(AgSR^t)_8$ cycle, something like **12** or **13** without the phosphine ligands, exists in solution.[5]

Acknowledgment. Support of this work by the Australian Research Grants Scheme is gratefully acknowledged.

Registry No. **8**, 119567-67-8; **9**, 119567-70-3; **10**, 119567-71-4.

Supplementary Material Available: Listings of full crystallographic details for **8–10** (Table S1), substituent dimensions for **8–10** (Tables S2–S4), and atom positional parameters and thermal parameters for **8–10** (Tables S5–S7) (14 pages); listings of observed and calculated structure factors for **8–10** (Tables S8–S10) (43 pages). Ordering information is given on any current masthead page.

(24) Gambarotta, S.; Floriani, C.; Chiesi-Villa, A.; Guastini, C. *J. Chem. Soc., Chem. Commun.* **1983**, 1087.

(25) dppm is bis(diphenylphosphino)methane: Khan, M. A.; Kumar, R.; Tuck, D. G. *Polyhedron* **1988**, *7*, 49.

(26) Dance, I. G.; Herath Banda, R. M. In preparation.